ISSN 1993-9973, e-ISSN 2415-332X

Vol. 25, No. 2
2025

PROSPECTING AND DEVELOPMENT OF OIL AND GAS FIELDS

https://pdogf.com.ua/en

Received: 15.07.2025. Revised: 03.11.2025. Accepted: 08.12.2025. Published: 09.01.2026.

UDC 622.276.53.054

DOI: 10.63341/pdogf/2.2025.36

Kinematic analysis of the characteristics of a crank-pulley rocking machine

Viktor Kharun*

PhD in Technical Sciences, Associate Professor
Ivano-Frankivsk National Technical University of Oil and Gas
76019, 15 Karpatska Str., Ivano-Frankivsk, Ukraine
https://orcid.org/0000-0003-1422-6003

Vasyl Popovych

PhD in Technical Sciences, Associate Professor
Ivano-Frankivsk National Technical University of Oil and Gas
76019, 15 Karpatska Str., Ivano-Frankivsk, Ukraine
https://orcid.org/0000-0003-2438-8532

Ivan Petryk

PhD in Technical Sciences, Associate Professor
Ivano-Frankivsk National Technical University of Oil and Gas
76019, 15 Karpatska Str., Ivano-Frankivsk, Ukraine
https://orcid.org/0000-0003-0863-5476

Zinovii Odosii

PhD in Technical Sciences, Professor
Ivano-Frankivsk National Technical University of Oil and Gas
76019, 15 Karpatska Str., Ivano-Frankivsk, Ukraine
https://orcid.org/0000-0003-0914-2489

Abstract. Oil production enterprises in Ukraine mainly use traditional balance drives, which have proven their reliability over many years of operation. New drive schemes, in terms of efficiency, require a comparative assessment of their characteristics with balance drives. For the purpose of comparative analysis and calculation of the kinematic parameters of the crank-pulley drive, which was operated at the Oil and Gas Production Department Okhtyrkanaftogaz of the Public Joint Stock Company Ukrnafta from 1993 to 2021, the paper presents the development of its mathematical model. For this purpose, geometric dependencies were used to calculate the length of the rope, which acts as a flexible link, and, accordingly, the displacement of the rod suspension. By differentiating the displacement graph, the corresponding kinematic characteristics were obtained – velocities and accelerations, which are components for calculating the moment of resistance forces reduced to the crank of the executive mechanism. The coefficients of mean square deviation calculated for traditional sucker-rod pumping units and crank-pulley drives allowed a comparative assessment of their balancing quality. Their characteristics were compared based on the load of the executive mechanism using a typical static dynamogram, since the accepted rotation speed of the crankshaft of sucker-rod pumping unit is less than 8 rpm. It was determined that the root mean square deviation of the torque of the crank-pulley drive was 9.47 kN×m, which is 33.6% less than that of a traditional balancing drive. Using a developed mathematical model, which employs the vector contour method, a system of linear equations was obtained to determine the dependence of the rotation angle φ_2 of the lower crossbar, to which the rope is attached, and the rotation angle φ_3 of the movable pulley on the rotation angle φ_1 of

Suggested Citation: Kharun, V., Popovych, V., Petryk, I., & Odosii, Z. (2025). Kinematic analysis of the characteristics of a crank-pulley rocking machine. *Prospecting and Development of Oil and Gas Fields*, 25(2), 36-47. doi: 10.63341/pdogf/2.2025.36.

*Corresponding author

the crank. It has been established that the movable pulley changes its direction of movement twice per revolution of the crank of the executive mechanism, which may be the cause of accelerated wear of the drive rope

Keywords: root mean square deviation; downhole rod pump unit; mathematical model; pump drive; reduced torque

Introduction

During 1993-2021, the Oil and Gas Production Department (OGPD) Okhtyrkanaftogaz of the Public Joint Stock Company (PJSC) Ukrnafta operated sucker-rod pumping units with a crank-pulley drive, which were later decommissioned due to the complexity of their maintenance. Most commonly, these sucker-rod pumping units are designed with a double-arm balancer. There are many types of executive mechanisms based on this design, which differ in the length of the front and rear arms (beams) of the balancer and other geometric dimensions. Despite the long period of use of such drives, researchers are working on improving their design methods.

J. Wang *et al.* (2025) proposed a new design scheme for the executive mechanism of a double-arm balancing drive by sequentially optimising both their kinematic and dynamic characteristics. The effectiveness of the new design was compared by calculating the root mean square value of the torque. Researchers J. Xu *et al.* (2022) improved the method of balancing a downhole rod pumping unit (DRPU) equipped with a double-arm balancer drive. The modified design of the executive mechanism, due to the placement of secondary balancing counterweights rotating at double angular velocity, made it possible to avoid changing the sign of the crank torque, which reduced the energy consumption of the drive electric motor.

Z.W. Gao & S. Jia (2024) conducted a review of methods for modelling and controlling balance drives and their mathematical models. It was determined that comparisons of the effectiveness of different methods should be based on comparisons with a reference mathematical model. Scientists A. Malyar & S. Cieslik (2023) developed mathematical models of a balance drive to calculate the process of changing the capacity of cosine capacitors to compensate for reactive power in the starting and steady states of an electric drive of DRPU. As a result, the change in the sign of the crankshaft torque was compensated by adjusting the capacitance of the capacitors.

In the publication by A.M. Aliyev & S.Y. Aliyeva (2023), the mathematical model of the DRPU was expanded in terms of modelling the processes of downhole equipment, in particular the stress-strain state of the valve assembly of a well pump. The influence of friction forces on the deformation and destruction of rods was determined, taking into account the kinematics of the rod string. The geometry of the DRPU drive usually includes several of the most common types of drives (sucker-rod pumping units) such as: traditional double-arm or single-arm balance drives with counterweights placed on cranks, called sucker-rod pumping units, long-stroke drives, which are used for significant lengths of well pump stroke (GE Oil & Gas, n.d.).

The situation is no different in Ukrainian fields. According to research by V.V. Savchuk (2016), ten oil fields were developed at the Dolyna Naftogaz Oil and Gas Production Company with an operational fund of 392 production wells, with an average depth of 2,700 metres. All major fields are in the late stages of development, which is characterised by high water cut – over 86%. More than 70% of wells are operated using balance drives. For wells with high oil flow rates, the use of non-balancing long-stroke DRPU drives (Weatherford, n.d.) is proposed, the design of whose executive mechanisms differs from that of balancing drives. In addition, the search for a replacement for the balancing drive with other executive mechanism schemes, for example, through the use of a hydraulic drive, continues. To determine the technical condition of DRPU equipment, the most common method remains the dynamographic method, which is constantly being improved. Based on this method, models are being developed for diagnostics, taking into account the actual dynamic level of fluid in the well in order to determine the energy of the oil and gas reservoir for selecting the necessary operating modes of sucker-rod pumping units (Zhang *et al*., 2021).

Analysis of scientific research allows to conclude that analytical calculations according to the developed mathematical models of traditional balance drives can be used as a basis for comparing the kinematic and dynamic characteristics of other drive schemes. Given the originality of the design of the crank-pulley drive executive mechanism and the absence of publications by Ukrainian researchers that theoretically confirm the advantages or highlight the disadvantages of such a drive scheme for DRPU, the purpose of this study was to calculate the kinematic parameters of the developed mathematical model for comparative evaluation with similar balance drives.

Materials and Methods

The structural diagram of the unbalanced crank-pulley drive of a well rod pump (DPCP) is shown in Figure 1. The DPCP operates as follows. Crank 1 rotates at an angular velocity ω_1 around the standpipe O and drives the tension pulley 2, which is covered by rope 3 thrown over the guide pulley 4. At point E, the rope is attached to the rod suspension 5, and at O_2 to a fixed link. Crank 1 has an L-shape, with a guide pulley hinged to one end, at A, and crank counterweights located at the other end, deflected by an angle α, at point B. When the crank rotates around the stand O, it pushes the tension pulley 2, which begins to move the rope 3, simultaneously rotating at an angular velocity ω_2. The movement of the rope is transmitted to the guide pulley 4, which rotates around the stand O_1 at an angular velocity ω_3, changing the direction of the rope's movement to vertical and, thus, the rod suspension E together with the rod string performs a translational movement, which is transmitted to the plunger of the deep well pump 7, which is located

in the pump-compressor pipe string 8. The weight of the rod string and the liquid above the plunger of the deep well pump is balanced by counterweights 9 located on the crank. During the operation of the rocker machine, the plunger 7 of the deep pump performs a reciprocating motion, moving from the extreme lower to the extreme upper position. The stroke of the plunger h is defined as the difference in the displacement of the rod suspension between its two extreme positions, which are defined by E_0 and E' (Fig. 2).

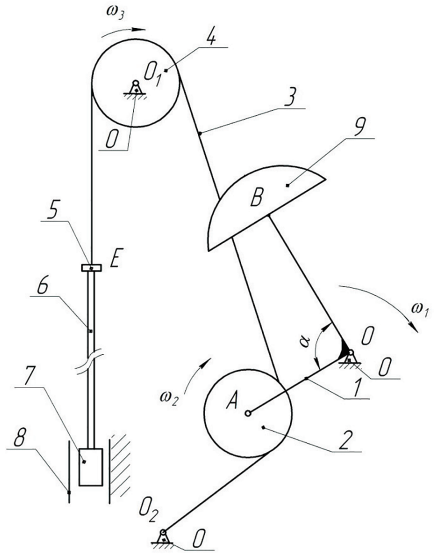

Figure 1. Structural diagram of DPCP

Note: 0 – fixed link (frame to which other moving links are attached); 1 – crank; 2 – tension (moving) pulley; 3 – rope; 4 – guide pulley; 5 – rod suspension; 6 – rod string; 7 – deep well pump plunger; 8 – tubing string (TS); 9 – crank counterweights
Source: developed by the authors based on Osnastka NPP (2001)

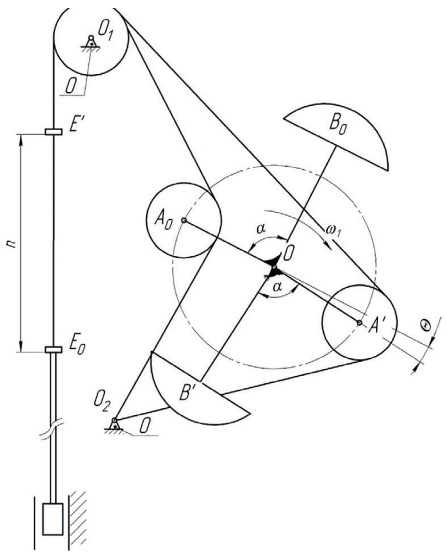

Figure 2. Extreme positions of the DPCP executive mechanism

Source: developed by the authors based on Osnastka NPP (2001)

The dimensions of the links are selected in such a way that between the extreme positions of the crank, which are determined by the lengths of segments OA_0 and OA', an angle of misalignment Q is formed, which allows the average speed of the rod suspension to be redistributed – reducing its value for the working stroke (upward movement of the rod suspension). This angle is calculated using the formula:

$$\theta = 180 \times \frac{k_v - 1}{k_v + 1}, \quad (1)$$

where k_v – crank average speed variation coefficient.

$$k_v = \frac{V_{up}}{V_d}, \quad (2)$$

where V_{up}, V_d – average speed of the rod suspension for its upward and downward movement. To compare the capabilities of this drive with traditional sucker-rod pumping unit, a mathematical model was created (Fig. 3), which was used to calculate the kinematic characteristics. For ease of reading the diagram, the part of the crank with counterweights is not shown.

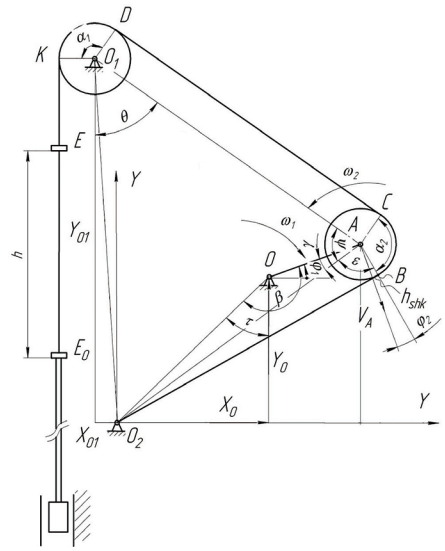

Figure 3. Calculation scheme of the executive mechanism
Source: developed by the authors

The displacement of the rod suspension h is calculated as the difference in rope length between its lower and upper extreme positions (E):

$$S_k = l_k - l_{k0}, \quad (3)$$

where l_k, l_{k0} – the, rope length in the arbitrary and initial (extreme) position of the crank:

$$l_k = O_2B + BC + CD + DK + KE, \quad (4)$$

where O_2B – the length of the rope between the standpipe and point B where the rope contacts the movable pulley.

$$O_2B = \sqrt{O_2A^2 - AB^2}, \quad (5)$$

where $AB = r_{shk}$ – the radius of the moving pulley. The length of the rope between A and B at the point where it attaches to the pulley is variable and depends on the position of the crank OA:

$$O_2A = \sqrt{(X_O + X_A)^2 + (Y_O + Y_A)^2}, \quad (6)$$

where X_O, Y_O – the projection of coordinate O on axes X and Y; $X_A = rkr \times \cos(\varphi_1)$ – the projection of crank length r_{kr} on axis X; $Y_A = r_{kr} \times \sin(\varphi_1)$ – the projection of crank length r_{kr} on axis Y; φ_1 – the crank rotation angle, calculated relative to the positive direction of axis X. Length of rope covering the movable pulley on the arc BC:

$$BC = r_{shk} \times \alpha_2, \quad (7)$$

where α_2 – the angle of rope coverage of the movable pulley.

$$\alpha_2 = \frac{3}{2} \times \pi - \varepsilon - \psi, \quad (8)$$

where $\varepsilon = \tan^{-1}\left(\frac{O_2B}{r_{shk}}\right)$; $\psi = \cos^{-1}\left(\frac{O_2A^2 + O_1A^2 - O_1O_2^2}{2 \times O_2A \times O_1A}\right)$, where $O_1O_2 = \sqrt{X_{01}^2 + Y_{01}^2}$. The length of the rope between points DC is equal to the length:

$$A = \sqrt{(Y_{O1} - Y_A)^2 + (X_O + X_A)^2}. \quad (9)$$

Length of rope covering the guide pulley:

$$DK = (\pi - \theta) \times r_{shk1}, \quad (10)$$

where r_{shk1} – the radius of the fixed pulley. The length of the rope in the initial position is calculated according to Figure 2, when point A of the crank is in such a position that the length of the rope l_k is minimal. By performing numerical differentiation of this graph, the dependence of the rod suspension speed is obtained, which is a component for calculating the reduced moment acting on the crankshaft. However, a special feature of this executive mechanism is that the DPCP drive contains a movable pulley 2, which changes the direction of its rotation several times during one revolution of the crankshaft, so this must be taken into account when constructing a mathematical model. To determine the dependence of the angular velocity of the movable pulley on the angle of rotation of the crank 1, the vector contour method was used, the calculation scheme of which is shown in Figure 4.

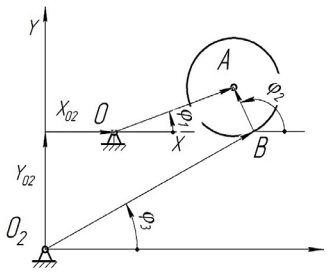

Figure 4. Vector contour for determining the kinematic parameters of a moving pulley

Source: developed by the authors

Equation of a vector contour:

$$\vec{l}_{OA} = \vec{X}_{O2} + \vec{Y}_{O2} + \vec{l}_{O2B} + \vec{l}_{AB}. \quad (11)$$

Projections on the axis to determine the unknowns φ_2 – the angle of rotation of the moving pulley and φ_3 – the angle of rotation of the rope:

$$\begin{cases} l_{OA} \times \cos\varphi_1 = -X_{02} + l_{O2B} \times \cos\varphi_3 + l_{AB} \times \cos\varphi_2 \\ l_{OA} \times \sin\varphi_1 = -Y_{02} + l_{O2B} \times \sin\varphi_3 + l_{AB} \times \sin\varphi_2 \end{cases}. \quad (12)$$

Solving the system of equations (12) allows obtaining the dependence of the angle of rotation φ_3 of the lower crossbar to which the rope is attached at O_2 and the angle of rotation φ_2 of the movable pulley. Differentiating equation (12) with respect to time t, the expressions for determining the angular velocities ω_2 and ω_3 are found:

$$\begin{cases} -l_{OA} \times \sin\varphi_1 \times \omega_1 = -l_{O2B} \times \sin\varphi_3 \times \omega_3 - l_{AB} \times \sin\varphi_2 \times \omega_2 \\ l_{OA} \times \cos\varphi_1 \times \omega_1 = l_{O2B} \times \cos\varphi_3 \times \omega_3 + l_{AB} \times \cos\varphi_2 \times \omega_2 \end{cases}. \quad (13)$$

The power of the drive motor depends on the shape of the torque curve acting on the drive crankshaft. Therefore, the next task was to determine the reduced torque acting on the crankshaft, taking into account the placement of crankshaft counterweights on it, which is determined according to the equation:

$$M_{zv}^0(\varphi_1) = M_F(\varphi_1) + M_{kr}(\varphi_1) + M_{pr}(\varphi_1), \quad (14)$$

where $M_F(\varphi_1)$ – the moment reduced to a crank from the force of useful resistance acting at the point of suspension of the rods; $M_{kr}(\varphi_1)$ – the moment created by the mass of the crank; $M_{pr}(\varphi_1)$ – the moment created by the masses of crank counterweights.

$$M_{zv}^0(\varphi_1) = F_{ko} \times \frac{V_E}{\omega_1} \times \cos\alpha_1 + \left(G_{shk} + \frac{1}{2} \times G_{kr}\right) \times \times l_{OA} \times \cos\varphi_1 + G_{bpr} \times l_{spr} \times \cos(\varphi_1 - \alpha), \quad (15)$$

where F_{ko} – the force of useful resistance acting on the bar suspension; V_E – the speed of the point of application of the force of useful resistance; ω_1 – the angular velocity of the crank; α_1 – the angle between the direction F_{ko} and velocity V_E; G_{shk} – the pulley weight; G_{kr} – the crank weight; G_{bpr} – the weight of counterweights; l_{spr} – the distance to the centre of mass of the counterweights; α – the angle between crankshaft beams. The components of the combined moment of resistance forces are shown in Figure 5.

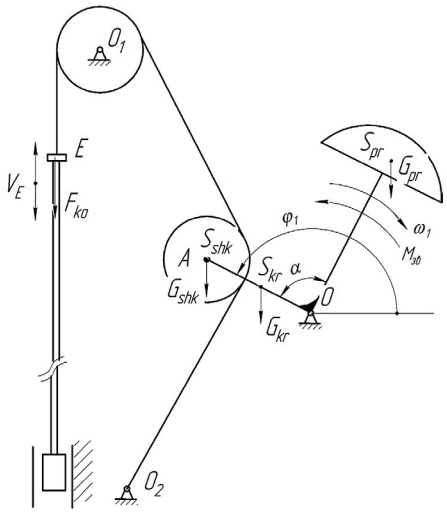

Figure 5. Components of the combined moment of resistance forces

Source: developed by the authors

In this case, the value of the useful resistance force is calculated taking into account the displacement of the rod suspension in accordance with the calculation scheme developed above (Fig. 3) for the upward (16) and downward (17) movement of the rod suspension:

$$\begin{cases} F_{ko} = \left(F_{min} + (F_{max} - F_{min}) \times \frac{S_E}{\lambda_1}\right) \times S_E \le \lambda_1 \\ F_{ko} = F_{max} \times \lambda_1 \le S_E < H; \end{cases} \quad (16)$$

$$\begin{cases} F_{ko} = \left(F_{max} - (F_{max} - F_{min}) \times \frac{H - S_E}{\lambda_1}\right) \times S_E \ge H - \lambda_2 \\ F_{ko} = F_{min} \times S_E < H - \lambda_2, \end{cases} \quad (17)$$

where H – stroke E of the rod suspension. For a dynamic dynamogram, the values F_{min} and F_{max} are calculated taking into account the acceleration of point E of the rod suspension:

$$\begin{cases} F_{min}^{d} = F_{min} \times a_E \\ F_{min}^{d} = F_{max} \times a_E, \end{cases} \quad (18)$$

where a_E – the acceleration of the rod suspension. The criterion for comparing the efficiency of balancing the DRPU drives is the coefficient of the root mean square deviation of the torque, which is calculated using the formula V.R. Kharun *et al*. (2021):

$$\sigma_M = \sqrt{\frac{\int_0^{2\pi} M_{zv^2} \times d\varphi_1}{2 \times \pi}}, \text{ H×m}, \quad (19)$$

where M_{zv} – the crank-reduced moment of resistance forces; φ_1 is the crank rotation angle.

Results and Discussion

Further on, a comparative analysis of the developed mathematical model of the DRPU crank-pulley drive with known analogues is presented, and its kinematic, dynamic and energy characteristics are considered in order to evaluate the efficiency and quality of the drive balancing. The manufacturers of the DPCP drive have determined that the unique geometry of this executive mechanism allows it to consume 1.5 times less electricity compared to a traditional balance drive (Osnastka NPP, 2001). However, these drives have not found wide application. The most widely used balancing drive in the world, the sucker-rod pumping unit, continues to be used in oil fields, accounting for more than 80% of oil production. To compare the capabilities of the drive with traditional sucker-rod pumping units, a mathematical model was created.

A similar mathematical model of a sucker-rod pumping unit with a crank-pulley drive, in which the crank with a drive pulley located on it is positioned with a certain eccentricity relative to another crank on which balancing counterweights are installed, was developed by researchers J. Xu *et al.* (2024). The drive scheme of these authors differs from the one considered in this article in that the counterweights are located on separate cranks, the axis of rotation of which coincides with the axis of rotation of the cranks with a movable pulley, but is located at a certain distance. This made it possible to improve the balance of the drive. In this mathematical model, the displacement of the rod suspension is determined by calculating the change in the length of the rope driven by the movable pulley, similar to the article presented, but the kinematics of the movable pulley is not taken into account. The researchers tested the prototype in the field, which allowed them to conclude that this design reduced the power of the drive motor by 80%, reduced the weight of the drive by 25%, and saved more than 50% of electricity. Thus, the advantage of such drives over traditional sucker-rod pumping units has been determined.

The mathematical model of the DPCP developed in this publication made it possible to determine the displacement of the rod suspension according to formula (3), determining the difference in rope lengths for the upper and lower positions of the rod suspension, similar to the model by J. Xu *et al*. (2024). However, it differs in the rope direction scheme from the drive (moving) pulley to the guide pulley, and this model additionally takes into account the kinematics of the moving pulley. The first kinematic characteristic that makes it possible to evaluate the correctness of the mathematical model is the displacement of the rod suspension. An example of constructing graphs of the dependence of the displacement of point E – the rod suspension – on the angle of rotation of the crank for different stroke lengths is shown in Figure 6.

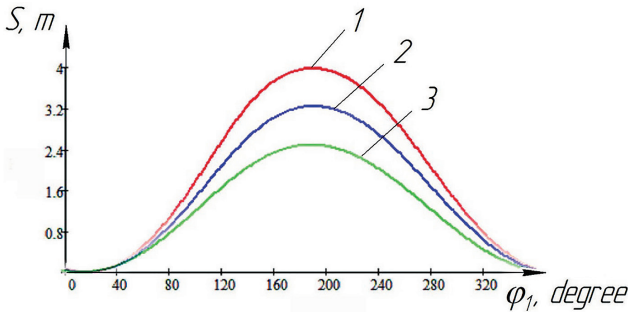

Figure 6. Stroke graphs for different plunger stroke lengths

Note: 1 – 4 m; 2 – 3 m; 3 – 2.5 m

Source: developed by the authors

The graph showing the dependence of the displacement of the suspension point of the rods on the angle of rotation of the crank is used by researchers to compare the differences between the proposed models of new executive mechanisms of DRPU drives and traditional balance drives. The authors J. Shao *et al.* (2021) developed an DRPU drive using a gear rack mechanism to transfer motion to the rod suspension. To confirm the difference in the movement of the rod suspension, they constructed a graph of the movement of the rod suspension of their proposed drive, along with a graph of a traditional sucker-rod pumping unit.

Displacement graphs are used not only to compare the performance of new drive models, but also to select the most efficient design for existing balance drives. B. Wang (2021) proposed an improved DRPU balance drive scheme with dynamic balancing tracking. The advantages of this scheme, compared to balance drives, were determined using displacement, velocity, and acceleration

graphs of the rod suspension point. Similarly, in this work, three displacement graphs of the rod suspension were constructed, which made it possible to evaluate the nature of displacement changes for different stroke lengths.

The developed mathematical model made it possible to compare the nature of the displacement change of the rod suspension. For this purpose, a comparison was made with a traditional balance drive with a rod suspension stroke of 3 m (Fig. 7). The maximum displacement of the rod suspension is 3 m, while for a traditional sucker-rod pumping unit, the crank rotation angle is 187°, and the desaxial angle is 7°, while in the DPCP drive, the rotation angle is 189°, i.e., the desaxial angle is increased to 9°. The desaxial angle characterises the duration of the working and idle strokes. Increasing the duration of the working stroke, during which the maximum load is applied to the rod suspension, allows for a more even distribution of the load on the drive.

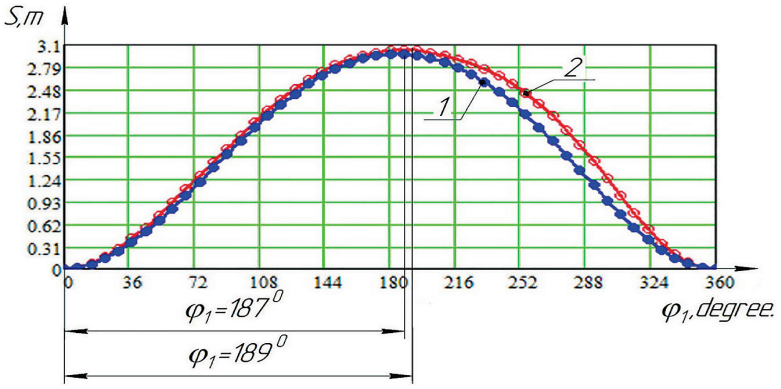

Figure 7. Rod suspension movement graphs for a stroke length of 3 m
Note: 1 – traditional balance drive; 2 – drive with DPCP
Source: developed by the authors

The dependence of the speed of the rod suspension can be obtained by differentiating the displacement, which can be done using analytical methods, as used by A.M. Aliyev & S.Y. Aliyeva (2023) and J. Wang *et al.* (2025), or numerical methods (Han *et al.*, 2025). Figure 8 shows the graphs of the speed of the rod suspension of a traditional balance drive and a crank-pulley drive, constructed by numerical differentiation of the displacement graphs, for the same crank rotation speed of 6.5 rpm.

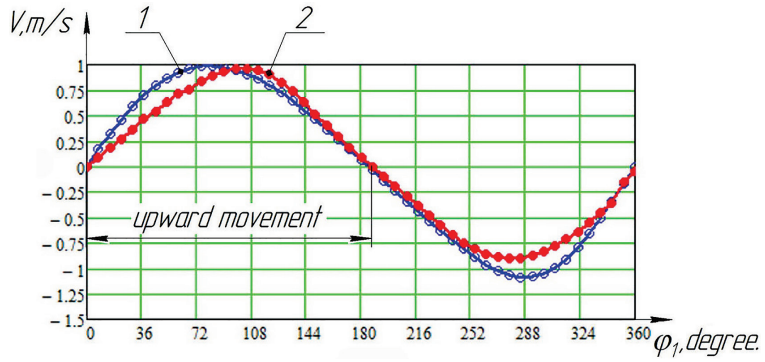

Figure 8. Rod suspension speed charts for a stroke length of 3 m
Note: 1 – traditional balance drive; 2 – drive with DPCP
Source: developed by the authors

Comparing speed graphs shows the advantages of new designs over traditional balance drives. From the analysis of these graphs (Fig. 8), it can be concluded that for a traditional sucker-rod pumping unit, the maximum speed value corresponds to 0.99 m/s for the upward stroke of the rod suspension and 1.08 m/s for the downward stroke. Accordingly, for a crank-pulley drive, the speed value for upward movement will be 0.96 m/s, which is close to the traditional value, but for downward movement it reaches 0.9 m/s. That is, for the DPCP drive, the difference in speeds for upward and downward movement will be smaller. Since the power at the rod suspension point is the product of speed and useful resistance force, the smaller the speed fluctuation, the lower the power consumption of the drive. Figure 9 shows the acceleration graphs of the suspension point of the rods of a traditional balance drive and a DRPU crank-pulley drive. Acceleration is a component of inertial force, which can be calculated using formula (18).

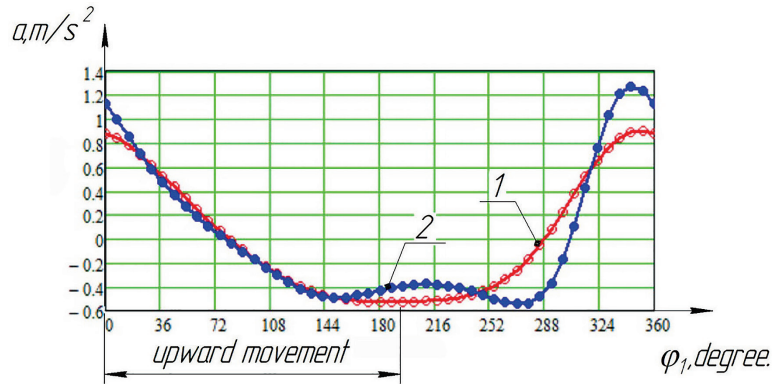

Figure 9. Acceleration graphs for rod suspension for a stroke length of 3 m

Note: 1 – traditional balance drive; 2 – drive with DPCP
Source: developed by the authors

Comparing the graphs, it can be seen that for the crank-pulley drive, the acceleration value is 20% lower at the beginning of the rod suspension's upward movement, but when the crank rotates by 22°, it actually equals the acceleration of a traditional balance drive. Also, at the end of the second phase of movement, when the rod suspension moves down, the acceleration value is also 26% lower than that of a traditional balance drive, which increases when the crank rotates from 324° to 360°. The developed mathematical model allows calculating the angular velocity of the moving pulley and the lower crossbar (Fig. 10), to which a rope is attached at point O_2 (Fig. 3).

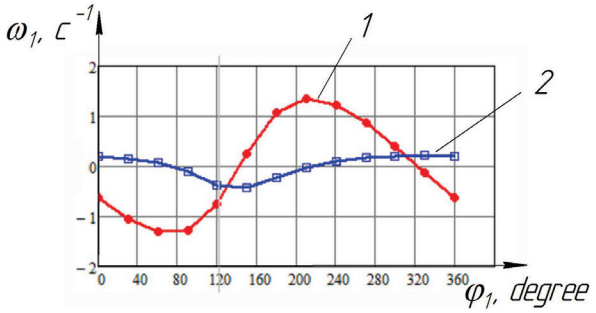

Figure 10. Angular velocities of the moving pulley 1 and the lower crossbar 2

Source: developed by the authors

Analysing the graphs, it can be noted that the angular velocity of the moving pulley changes the direction of its rotation twice per crank revolution and reaches 1.3 rad/s. Since the drive pulley is in contact with the rope, the movement of which is transmitted to the rod suspension, the change in the direction of movement leads to a similar change in the direction of the friction force, and this can cause increased rope wear. In formula (15), the effective resistance force F_{ko} is a mechanical characteristic (dynamogram) that shows how the force acting on the rod suspension changes depending on the displacement of point E of the rod suspension. The graph of this force is the basic component for balancing the sucker-rod pumping unit (Takacs & Kis, 2021).

In the work of R. Zhang *et al*. (2021), a study was conducted on the influence of the condition of the downhole pump on the shape of surface and downhole dynamograms. It was noted that the shape of the dynamogram depends on the dynamic level of fluid in the well, the presence of gas, rod breakage, high or low plunger seating of the deep well pump, and other conditions of deep well equipment. F.C. de Oliveira & O.J. Romero (2024) modelled dynamograms to evaluate the strategy for optimising production processes in DRPU oil production. These researchers compared dynamograms with a theoretical (static) dynamogram, which does not take into account the dynamic loads caused by the acceleration and vibration of the links.

A dynamic dynamogram (Fig. 11, curve 2), which takes into account the acceleration of the rod suspension (18), has a certain effect on the shape of the torque, as noted in the studies by G. Takacs & L. Kis (2021), so this must be taken into account in order to achieve a better balance of the balance drive. Scientists note that traditionally, most researchers do not take into account the influence of inertial forces on the torque of the crankshaft. Figure 11 shows a static dynamogram that was modelled for the design of a rod string, taking into account the deformation of the rods and the pump-compressor pipe string when they are subjected to the load from the weight of the fluid (Fig. 11, curve 1) according to formulas (16-17) and a dynamic dynamogram, using the formula (18).

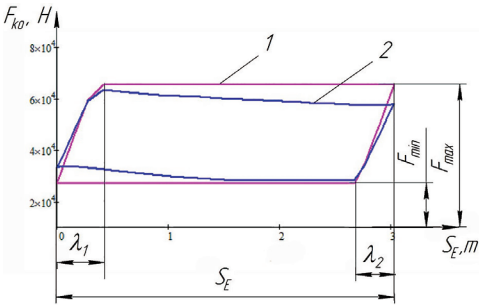

Figure 11. Typical dynamograms

Note: 1 – static; 2 – dynamic
Source: developed by the authors

For both dynamograms, it is possible to identify characteristic sections where the maximum load F_{max} acts, caused by the rod suspension perceiving the static load of the rod string and the fluid above the plunger, and the minimum load F_{min}, the main component of which is the weight of the rod string. During the transfer of load from the pump-compressor pipe column to the rod column, they are deformed by an amount λ_1 during the upward movement of the rod suspension and reverse deformed by an amount λ_2 during its downward movement. Since, according to Figure 9, the acceleration graphs of the balance and crank-pulley drives practically coincide in the phase of the rod suspension's upward movement, when the maximum load is applied to the drive, and most authors use a static dynamogram for kinematic analysis, it was decided to calculate the torque of the crank shaft using a static dynamogram.

Authors Z.W. Gao & S. Jia (2024) conducted a comparative analysis of the works of researchers who studied intelligent methods of controlling DRPU. It is noted that most of them focused on controlling the drive motor (52%) and the well fluid pumping system (34%), respectively. The main works concerned increasing the efficiency of the installation as a whole (31% of scientific publications) and reducing the power of the electric motor (28% of works), 16% on controlling the torque of the electric motor, 12% on the speed of pumping fluid from the well, and 13% on controlling the speed of rotation of the electric motor shaft. These findings are confirmed by researchers T.A. Aliev *et al.* (2022), who conducted early diagnostics of the technical condition of the DRPU equipment and controlled the drive electric motor using frequency converters.

The authors B. Ahmedov *et al.* (2023) claim that when switching from a balanced pump unit to an unbalanced one, the efficiency coefficient (EC) decreases from 83.4% to 65%. Similarly, researchers A. Malyar & M. Malyar (2025) combined the optimisation of the DRPU, choosing the torque of the crank and the delivery coefficient of the deep well pump as the optimisation criteria. Other scientists, D. Feng *et al.* (2022), created a parametric model of a balance drive and optimised it by developing a neural network in which one of the optimisation factors was the torque of the crankshaft. Therefore, in the presented DPCP model, this parameter was selected for the study, the graph of which was obtained as the result of two torques reduced to the crank – from the force of useful resistance $M_F(\varphi_1)$ and the moment of crank counterweights $M_{pr}(\varphi_1)$. The graphs of these moments, which are included in formula (15), calculated for the crank-pulley drive are shown in Figure 12.

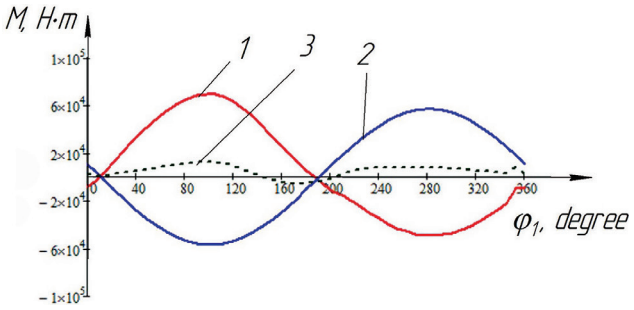

Figure 12. Moment graphs

Note: 1 – $M_F(\varphi_1)$; 2 – $M_{pr}(\varphi_1)$; 3 – $M_{zv}(\varphi_1)$
Source: developed by the authors

As can be seen from the analysis of the graph of the resulting torque $M_{zv}(\varphi_1)$, when the crank rotates from 0 to 150°, the torque is positive, from 150° to 205° it is negative, and from 205° to 360° it is positive again. Thus, the crank-pulley drive scheme cannot avoid a change in the sign of the torque, which is a negative factor in the operation of the drive. The same conclusion was reached by B. Ahmedov *et al.* (2021), who studied the balancing of the DRPU unbalanced drive and noted the presence of a negative part of the torque, which leads to shocks in the gear transmission of the reducer, increased wear and tear, and tooth breakage. As a result, it is impossible to completely eliminate this phenomenon, so efforts should be made to limit the magnitude of the negative torque by means of high-quality balancing.

The presence of a negative torque component was also noted by scientists in the work of G. Takacs & L. Kis (2021), which additionally investigated the influence of inertial forces and provided recommendations for improving balance, taking into account the position of the centre of mass of the counterweights, which leads to a reduction in both the negative part and the amplitude of the torque. It was noted that the traditional method of optimising torque, which consists of equalising its maximum values for the upward and downward movement of the suspension rods, does not ensure minimum power consumption of the drive motor. It is more expedient to use its root mean square deviation, and the smaller it is, the lower the required rated power of the motor.

Researchers A. Malyar & S. Cieslik (2023) noted that the negative part of the torque is the cause of the variable load of the DRPU drive, it is practically impossible to avoid this part, and it leads to the emergence of reactive power of the electric motor. The developed methodology made it possible to compensate for reactive power in the starting and steady-state modes of the electric drive. Comparative graphs of the crankshaft torque are presented in Figure 13, and the values of the root mean square deviation coefficients are given in Table 1.

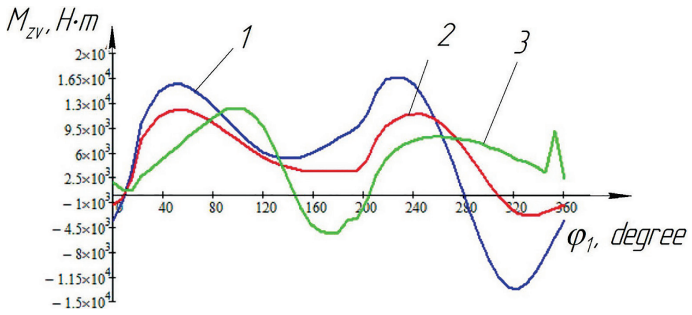

Figure 13. Graphs of combined moments of DRPU drives

Note: 1 – improved balance drive with a movable pulley; 2 – traditional balance drive; 3 – crank-pulley drive
Source: developed by the authors based on current research and V.R. Kharun *et al*. (2021)

According to comparative calculations, an improvement in balancing was obtained for the crank-pulley drive (Table 1), since the root mean square deviation coefficient decreased by 33.6% compared to the traditional balance drive. And, therefore, in accordance with the above considerations, this led to an increase in the efficiency of the entire DRPU. The results of the calculations are summarised in Table 1.

Table 1. Comparison of drive balancing quality assessment

Type of drive DRPU	Value σ_M, kN×m	Reduction of the root mean square deviation coefficient, %
Traditional balance UP12T-3-5500	14.26	-
The UP12T-3-5500-based balancer drive equipped with a movable pulley	10.54	26.1
Crank-pulley DPCP	9.47	33.6

Source: developed by the authors based on current research and V.R. Kharun *et al*. (2021)

It should be noted that although the calculation of the DPCP balance resulted in graph 3 with different values of the maximum moment during the upward movement of the rod suspension (crank rotation angle of 97°) and downward movement (rotation angle of 250°), the quality of its balancing is better (the root mean square deviation coefficient is 9.47 versus 14.26), which is consistent with the conclusions of G. Takacs & L. Kis (2021). The analysis of the root mean square deviation coefficient of the reduced moment of the crank shaft can be used in the development of adaptive control algorithms based on artificial intelligence, which was proposed by the author O. Turchyn (2025) for automatic regulation of the operating modes of the DRPU. Thus, the results of modelling and comparative analysis confirm the feasibility of using a crank-pulley drive, since the proposed mathematical model allows for an adequate description of kinematic and dynamic processes, improves the quality of balancing, reduces torque fluctuations, and creates the conditions for increasing the energy efficiency and reliability of the pump unit.

Conclusions

The developed mathematical model and comparative assessment calculations of balancing quality showed that the speed characteristics of the crank-pulley drive's executive mechanism allow it to operate with better performance than traditional balance drives, since the speed for the downward stroke of the suspension is 0.9 m/s compared to 1.08 m/s for a traditional balance drive, which is 20% less. The comparison of the displacement graphs of the rod suspension of a traditional balance drive and a crank-pulley drive should be performed relative to the extreme position of the rod suspension. One of the advantages of the latter is a larger desaxial angle, which has been increased to 9°, allowing for a reduction in the deviation of the speed and acceleration of the rod suspension point from its average value.

At the beginning of the stroke of the balance drive rod suspension, the acceleration exceeds the DPCP value by 20%, but when the crank rotates 22° relative to the extreme position, it evens out and practically coincides with the acceleration of the DPCP drive. At the end of the downward stroke of the rod suspension, which corresponds to a crank rotation angle of 324° to 360°, the acceleration of the balance drive again exceeds the value by 26%. This indicates that the dynamic characteristics of the DPCP drive are also better. Using a mathematical model, it has been determined that the operation of this drive is accompanied by a change in the direction of rotation of the drive pulley, twice per crank rotation its angular velocity reaches 1.3 rad/s. Accordingly, this negatively affects the durability of the flexible link – the rope, since the change in the direction of rotation leads to a change in the sign of the contact stresses at the point of contact between the rope and the pulley. A comparative analysis of traditional balance drives and new DRPU executive mechanism schemes can be carried out using a typical static dynamogram, since the acceleration graphs of the balance drive rod suspension and the DPCP drive coincide in the upward movement phase of the rod suspension when the maximum load is applied to the drive.

Intelligent control methods for rod pump units aimed at improving the efficiency of the DRPU oil extraction process

are mainly focused on controlling the characteristics of the drive motor – torque and shaft rotation speed. The torque of the drive motor, through the drive gear ratio, is related to the torque of the crankshaft, so by comparing the root mean square torque deviation coefficient, more efficient drives can be selected. In the study, the root mean square deviation coefficient of the DPCP drive is 9.47 kN/m, which is 33.6% less than in the balance drive, so it can be argued that the crank-pulley drive has better balancing performance.

The negative value of the crankshaft torque negatively affects the operation of the drive gearboxes and, for a well-balanced drive, is 12 kN×m and manifests itself at the end of the rod suspension stroke downwards during the crankshaft rotation angle from 280° to 360°, while for the crank-pulley drive it is significantly lower, amounting to 5 kN×m, and manifests itself at the end of the rod suspension stroke upwards during the crank rotation from 150° to 205°. Thus, based on the research conducted, it can be noted that the kinematic characteristics of the DPCP drive are better compared to traditional balance drives. Considering the significant service life of these drives, from 1993 to 2021, at the OGPD Okhtyrkanaftogaz PJSC Ukrnafta, it would be advisable in the future to conduct a technical assessment of the reasons for their problematic operation in order to further improve the design of unbalanced drives.

Acknowledgements

The authors express their sincere gratitude to Mykolai Chepula, former technical director of Osnastka NPP, who was involved in the manufacture of crank-pulley drives, for his assistance in obtaining information materials on these drives and providing ideas for writing this publication. Also, Oleksii Fesenko, Head of Technical Service at OGPD Okhtyrkanaftogaz PJSC Ukrnafta, for his assistance in evaluating the operational capabilities of sucker-rod pumping units with crank-pulley drives.

Funding

None.

Conflict of Interest

None.

References

[1] Ahmedov, B., Hajiyev, A., & Mustafayev, V. (2021). Estimation of the equality of the beamless sucker-rod oil pumping unit by the value of the consumption current. *Nafta-Gaz*, 9, 571-578. doi: 10.18668/NG.2021.09.01.

[2] Ahmedov, B., Khalilov, I., & Hajiyev, A. (2023). Evaluation of the energy efficiency of the new model of sucker-rod pumping unit. *Machine Science*, 2, 28-39. doi: 10.61413/DOVZ1701.

[3] Aliev, T.A., Guluyev, G.A., Rzayev, A.H., Aliyev, Y.G., Rezvan, M.H., Yashin, A.N., & Khakimyanov, M.I. (2022). Ways to increase the efficiency of sucker rod pump units in oil production. *Journal of Engineering Research and Sciences*, 1(3). doi: 10.55708/js0103001.

[4] Aliyev, A.M., & Aliyeva, S.Y. (2023). Influence of mechanical factors on the performance and aging process of oil pump jack. *Nafta-Gaz*, 12, 776-785. doi: 10.18668/NG.2023.12.03.

[5] de Oliveira, F.C., & Romero, O.J. (2024). Development of the Rodsim numerical simulator for the study of a sucker rod pump, comparing the Gibbs (1963) and Lea (1990) models. *Latin American Journal of Energy Research*, 11(1), 12-23. doi: 10.21712/lajer.2024.v11.n1.p12-23.

[6] Feng, D., Qi, Y., Yu, Y., & Zhu, H. (2022). Neural network-based beam pumper model optimization. *Computational Intelligence and Neuroscience*, 2022(1), article number 8562387. doi: 10.1155/2022/8562387.

[7] Gao, Z.-W., & Jia, S. (2024). Modeling and control for beam pumping units: An overview. *Processes*, 12(7), article number 1468. doi: 10.3390/pr12071468.

[8] GE Oil & Gas. (n.d.). *Lufkin beam pumping units*. Retrieved from https://www.geoilandgas.com/oilfield/artificial-lift-well-performance-services/lufkin-beam-pumping-units.

[9] Han, X., Zhao, P., Zhao, X., & Zi, B. (2025). Review on machine learning-based approaches for the kinematic analysis and synthesis of mechanisms. *Frontiers of Mechanical Engineering*, 20, article number 11. doi: 10.1007/s11465-025-0827-5.

[10] Kharun, V.R., Senchishak, V.M., Popovych, V.Ya., & Shostakivskyi, I.I. (2021). Comparative evaluation of the executive mechanism of beam pumping unit drive equipped with a long-stroke column. *Oil and Gas Power Engineering*, 2(36), 57-67. doi: 10.31471/1993-9868-2021-2(36)-57-67.

[11] Malyar, A., & Cieslik, S. (2023). Calculation of processes in the electric drive of the sucker-rod pumping unit with reactive power compensation. *Energies*, 16(23), article number 7782. doi: 10.3390/en16237782.

[12] Malyar, A., & Malyar, M. (2025). Optimization of pump jack electric drive operation taking into account reservoir flow rate. *Technology Audit and Production Reserves*, 1(81), 75-78. doi: 10.15587/2706-5448.2025.322457.

[13] Osnastka NPP. (2001). *Crank-sheave drive of the sucker-rod pump PKSh56-120-4: Non-counterbalanced pumping unit with crank-shtave converting mechanism. Passport*. Kramatorsk: Osnastka NPP.

[14] Savchuk, V.V. (2016). Oil production with high content of sand, asphaltenes and wax using special pump constructions. *Scientific Bulletin of Ivano-Frankivsk National Technical University of Oil and Gas*, 1(40), 20-29.

[15] Shao, J., Ding, K., & Wang, D. (2021). Kinematics analysis of incomplete gear and rack pumping unit. *Journal of Physics*: *Conference Series*, 2095, article number 012090. doi: 10.1088/1742-6596/2095/1/012090.

[16] Takacs, G., & Kis, L. (2021). A new model to find optimum counterbalancing of sucker-rod pumping units including a rigorous procedure for gearbox torque calculations. *Journal of Petroleum Science and Engineering*, 205, article number 108792. doi: 10.1016/j.petrol.2021.108792.
[17] Turchyn, O. (2025). Introduction of neural network technologies to optimise the control of the operating modes of a sucker-rod pump installation. *Machinery & Energetics*, 16(1), 32-42. doi: 10.31548/machinery/1.2025.32.
[18] Wang, B. (2021). Dynamic strength analysis of the key components of the beam-type pumping unit with dynamic tracking balance. *Fracture and Structural Integrity*, 15(57), 291-299. doi: 10.3221/IGF-ESIS.57.21.
[19] Wang, J., Guo, Q.-Y., Fu, C.-L., Dai, G., Xia, C.-Y., & Qian, L.-Q. (2025). A novel optimization scheme for structure and balance of compound balanced beam pumping units using the PSO, GA, and GWO algorithms. *Petroleum Science*, 22(3), 1340-1359. doi: 10.1016/j.petsci.2025.01.007.
[20] Weatherford. (n.d.). *Long-stroke pumping unit*. Retrieved from https://www.weatherford.com/products-and-services/production-and-intervention/artificial-lift-systems/reciprocating-rod-lift-systems/pumping-units/long-stroke-pumping-unit/.
[21] Xu, J., Li, W., & Meng, S. (2022). Kinematic and dynamic simulation analysis of modified conventional beam pumping unit. *Energies*, 15(15), article number 5496. doi: 10.3390/en15155496.
[22] Xu, J., Wang, W., Li, W., Zhu, Q., & Lu, H. (2024). Kinematic and dynamic analysis of eccentric balanced positive torque pumping unit. *Machines*, 12(4), article number 240. doi: 10.3390/machines12040240.
[23] Zhang, R., Yin, Y., Xiao, L., & Chen, D. (2021). A real-time diagnosis method of reservoir-wellbore-surface conditions in sucker-rod pump wells based on multidata combination analysis. *Journal of Petroleum Science and Engineering*, 198, article number 108254. doi: 10.1016/j.petrol.2020.108254.

Кінематичний аналіз характеристик кривошипно-шківного верстата-гойдалки

Віктор Харун

Кандидат технічних наук, доцент
Івано-Франківський національний технічний університет нафти і газу
76019, вул. Карпатська, 15, м. Івано-Франківськ, Україна
https://orcid.org/0000-0003-1422-6003

Василь Попович

Кандидат технічних наук, доцент
Івано-Франківський національний технічний університет нафти і газу
76019, вул. Карпатська, 15, м. Івано-Франківськ, Україна
https://orcid.org/0000-0003-2438-8532

Іван Петрик

Кандидат технічних наук, доцент
Івано-Франківський національний технічний університет нафти і газу
76019, вул. Карпатська, 15, м. Івано-Франківськ, Україна
https://orcid.org/0000-0003-0863-5476

Зіновій Одосій

Кандидат технічних наук, професор
Івано-Франківський національний технічний університет нафти і газу
76019, вул. Карпатська, 15, м. Івано-Франківськ, Україна
https://orcid.org/0000-0003-0914-2489

Анотація. Нафтовидобувні підприємства в Україні переважно використовують традиційні балансирні приводи, які впродовж багатьох років експлуатації підтвердили свою надійність. Нові схеми приводів, з точки зору ефективності, потребують проведення порівняльної оцінки їх характеристик з балансирними приводами. З метою порівняльного аналізу та розрахунку кінематичних параметрів кривошипно-шківного приводу, який експлуатувався в Нафтогазовидобувному управлінні «Охтирканафтогаз» Публічного акціонерного товариства «Укрнафта» з 1993 по 2021 рр., у роботі наведено розробку його математичної моделі. Для цього використано геометричні залежності, які дозволили розрахувати довжину канату, який виступає гнучкою ланкою, і відповідно, переміщення штангової підвіски. Диференціюючи графік переміщення отримано відповідні кінематичні характеристики – швидкості та пришвидшення, які виступають складовою для розрахунку моменту сил опору, зведених до кривошипа виконавчого механізму. Коефіцієнти середньоквадратичного відхилення, розраховані для традиційних балансирних верстатів-гойдалок та кривошипно-шківного приводу, дозволили провести порівняльну оцінку якості їх зрівноваження. Порівняння їх характеристик проведено за навантаженням виконавчого механізму типовою статичною динамограмою, оскільки прийнята швидкість обертання кривошипа верстатів-гойдалок є меншою за 8 об/хв. Визначено, що середньоквадратичне відхилення крутного моменту кривошипно-шківного приводу склало 9,47 кН×м, що на 33,6 % менше, ніж у традиційного балансирного приводу. За допомогою розробленої математичної моделі, у якій використано метод векторного контуру, отримано систему лінійних рівнянь для визначення залежності кута повороту φ_2 нижньої траверси, до якої кріпиться канат, та кута повороту φ_3 рухомого шківа від кута φ_1 повороту кривошипа. Встановлено, що рухомий шків змінює свій напрямок руху двічі за один оберт кривошипа виконавчого механізму, що може бути причиною пришвидшеного зносу привідного канату

Ключові слова: середньоквадратичне відхилення; свердловинна штангова насосна установка; математична модель; привід насоса; зведений момент